

Gaussian Condensation Filter Based on Cooperative Constrained Particle Flow

Ran Wang¹, Graduate Student Member, IEEE, Cheng Xu¹, Member, IEEE, Hang Wu¹, Yuchen Shi, Shihong Duan¹, and Xiaotong Zhang¹, Senior Member, IEEE

Abstract—Real-time high-accuracy localization has a wide range of applications in scenarios, such as pedestrian navigation, emergency rescue, and vehicle networks. In these conditions, the measurement models are often nonlinear, and traditional Kalman and particle filters cannot provide long-time high-precision location-based services. To this end, we propose a Gaussian condensation filter (GCF) algorithm that can achieve high-accuracy localization in a harsh environment. However, aiming at the degradation of sampling points in target tracking based on the GCF, this article proposes a GCF algorithm based on particle flow which transfers the sample points satisfying the prior distribution of the target state to the posterior distribution, thereby improving the practical accuracy of the target-tracking algorithm. Further, to enhance the information fusion in the cooperative network, we propose a multitarget cooperative tracking algorithm to accomplish spatially constrained timing filtering of state information for improving the error correction of the target nodes on timing estimation. Numerical simulations are conducted to determine the effectiveness of our proposed algorithms. Compared with the GCF, its positioning accuracy is improved to 44.6%. Compared with the Gaussian condensation algorithm based on particle flow (PF), the practical accuracy of the GCF algorithm based on cooperative constrained PF in multitarget tracking is improved to 58.1%.

Index Terms—Constrained optimization, cumulative error, Gaussian mixture distribution, multitarget tracking, nonlinear filter.

I. INTRODUCTION

REAL-TIME high-accuracy localization is a crucial component of the Internet of Things (IoT) applications, such as pedestrian navigation, search and rescue, and autonomous vehicles. In quite a few scenarios, the global positioning system (GPS) can provide sufficient accurate positioning technical support for general positioning requirements [1]. However, in harsh and complex industrial environments, GPS-based positioning technology is also challenging to meet practical application needs. Currently widely used wireless positioning technologies, such as time difference of arrival

(TDOA) [2], angle of arrival (AOA) [3], received signal strength indication (RSSI) [4], and time of arrival (TOA) [5], can provide a real-time accurate location estimation in areas that GPS signals cannot cover, but most require predeployment of base stations. The inertial navigation system based on the inertial measurement unit (IMU) can perform position estimation through its sequence data without the need to deploy additional communication base stations. However, the shortcoming of the IMU method is the accumulated error, which cannot provide long-term high-precision position estimation [6]. To overcome these limitations, Xu et al. [7] proposed a fusion method based on IMU/TOA, combining the characteristics of IMU measurement with instantaneous high precision and the attributes of TOA without accumulated error, which is a long-term and large-distance span.

The Bayesian filter is widely considered for multitarget tracking [1], [5]. It is a recursive filter in which each measurement is processed in turn, and the posterior distribution of the current state is computed based on the current measurements and the posterior distribution calculated at the previous state. It resembles an ordinary recursive filter (e.g., a Kalman filter) for single-target tracking. Still, there are two significant differences: 1) on the dynamic model aspect, the filter must compute the joint posterior of all target states, whose complexity grows without bound over time and 2) on the measurement model aspect, the likelihood function factors conditional on the association variable, and so the exact update step must sum over exponentially many possible associations. To reduce the computational complexity of multitarget tracking, the dynamic model is generally considered a Gaussian model [8], [9]. Even though based on the non-Gaussian hypothesis, it generally needs to reduce the dimensionality of the multitarget-tracking process by mapping it to Gaussian space for computation due to the complexity of data association [10]. However, the measurement model issue remains unsolved.

Most of the measurement models considered in the existing literature are also based on the Gaussian model assumption [9], [11]. However, in practical applications, the likelihood between different measurement pairs could differ significantly in cooperative target-tracking networks, generally resulting in a nonlinear and non-Gaussian mixture for the overall likelihood functions [5]. Due to the data association uncertainty, the filter step cannot be performed independently for the individual targets. Rosato et al. [12] proposed a particle filter based on Monte Carlo sampling, which only has good adaptability to the single-target tracking system of the nonlinear model but

Manuscript received 3 October 2022; revised 20 December 2022, 7 January 2023, and 30 January 2023; accepted 25 March 2023. Date of publication 28 March 2023; date of current version 25 July 2023. This work was supported in part by the National Natural Science Foundation of China under Grant 62101029. (Corresponding author: Cheng Xu.)

The authors are with the School of Computer and Communication Engineering and the Shunde Innovation School, University of Science and Technology Beijing, Beijing 100083, China (e-mail: wangran@xs.ustb.edu.cn; xucheng@ustb.edu.cn; wuhang@xs.ustb.edu.cn; shiyuchen@xs.ustb.edu.cn; duansh@ustb.edu.cn; zxt@ies.ustb.edu.cn).

Digital Object Identifier 10.1109/JIOT.2023.3262641

does not consider multitarget positioning. Therefore, there are still challenges in implementing a nonlinear fusion localization scheme in the measurement model.

You et al. [13] proposed the unscented Kalman filter (UKF), which can solve the problem of non-Gaussian random noise to a certain extent based on the approximate posterior distribution of deterministic sampling points. Before the introduction of the particle filter in the 1990s, Kalman-like filters have been widely used by default to solve many significant problems. Wang et al. [14] proposed a particle filter based on Monte Carlo sampling, which uses the mean value of a set of weighted particles to estimate the mean and covariance of the state, approximating the posterior distribution of the region containing the saliency probability. Still, it faces the problem of particle degradation and depletion in the resampling process. For low-dimensional problems, particle filter can achieve high-precision localization with the same complexity as EKF, but for high-dimensional issues [15], high complexity is often required. Aiming at the nonlinear problem of the measurement model, this article proposes a Gaussian condensation filter (GCF), which uses a Gaussian mixture model to approximate the posterior probability distribution.

To effectively suppress the cumulative error effects of autonomous navigation and positioning, network collaborative optimization techniques can be used to improve positioning accuracy. Facing the self-organizing and highly dynamic environment, collaborative technology can fuse the sensory information collected by individuals to obtain information gained among group target nodes. Specifically, in a cooperative network, a single target node receives position information from inertial measurement equipment and generates autonomous ranging information with other nodes in the wireless network. Based on this mutual information, they coordinate to complete the optimal estimation of target positioning. Mobile node devices only need to embed inertial measurement and ranging sensors to achieve multitarget co-location based on their inertial and spatial distance measurements. When we consider static space optimization, we only pay attention to the influence of the space measurement at the current moment on the optimization of the state estimation, and the constraints of the state can be obtained based on the distance measurement outside the node. The posterior state means under the distance constraint can be obtained in standard Bayesian methods. Fan et al. [16] proposed a co-localization technique that utilizes spatial location information to optimize tracking multiple target locations. However, the above-mentioned static distance fusion optimization method must deploy an external base station. The wireless signal is prone to non-line-of-sight occlusion (NLOS), which causes significant errors. In the research of this article, we apply the state mean value after distance constraint optimization to the filter estimation process of the time series and realize the cooperative target tracking that integrates the measurement information in the spatiotemporal domain to obtain the filter estimation that is closer to the actual position.

In summary, our main contributions are as follows.

- 1) Aiming at the nonlinear measurement model problem faced by the multitarget tracking, a GCF algorithm is proposed, which uses a Gaussian mixture model

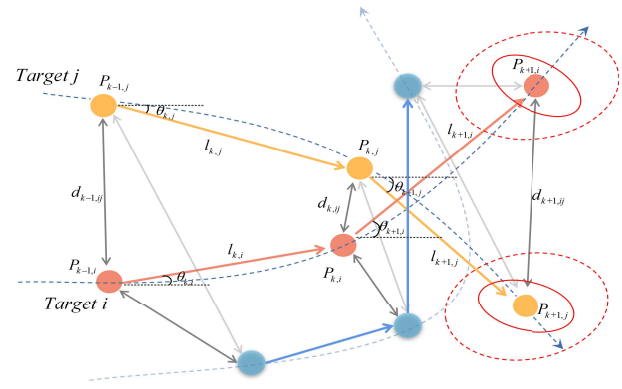


Fig. 1. Schematic of multitarget cooperative tracking: the internal inertial measurement of the target node is represented as a one-way arrow in the figure, and the external distance measurement is represented as a two-way arrow.

to approximate the actual posterior probability density function and can achieve high-precision positioning estimation in harsh environments.

- 2) Aiming at the problem of sampling point degradation in target tracking implemented by GCF, this study introduces particle flow (PF) into state estimation application scenarios. Through the PF mechanism, the state space sampling points satisfying the target state's prior distribution are transferred to the posterior distribution. Then the posterior probability samples are updated through Gaussian condensation to update the state variance, thus effectively solving the problem of sampling point degradation.
- 3) Given the cumulative error effect of Bayesian recursive filter, this study proposes a GCF based on collaborative constraints to optimize PF. Effectively improve the information fusion in the cooperative network.

The remainder of this article is organized as follows. Section II formulates the problem. Section III proposes a multiobjective cooperative GCF (CGCF). Section IV presents the simulation results. Section V summarizes the article.

II. PROBLEM DEFINITION

This section mainly describes the multitarget-tracking problem in 2-D scenarios as a case study to evaluate the algorithm's performance. This study considers that the target node can obtain intranode inertial and internode distance measurements. First, the multitarget dynamic model and sensor measurement model under cooperative conditions are established to perform multitarget tracking.

A. Dynamic Model

Fig. 1 shows the dynamic model-building process of the target node. Define that the cooperative network contains M moving target nodes. $\Omega = \{1, 2, \dots, M\}$ represents the set of target nodes. Assuming that each target node walks randomly in 2-D coordinates under discrete time $t_k (k \in [0, K])$. Define $X_{k,i} \in \mathbb{R}^3$ as the state information of target node i at time t_k , including position information $P_{k,i} = [px_{k,i}, py_{k,i}]^T$ and speed

information $V_{k,i}$, then X_k is expressed as

$$X_k = [P_{k,1:M}, V_{k,1:M}]^T. \quad (1)$$

For the time series changes, considering that the motion law of the target node conforms to the dynamic random walk process, the state of the target node is modeled according to the state information at the last moment and the heading angle measurement and estimation method. The state $X_{k,i}$ of the target node i at time t_k transfers to the state $X_{k+1,i}$ at time t_{k+1} , and establish the following dynamic model:

$$X_{k+1,i} = \begin{bmatrix} px_{k+1,i} \\ py_{k+1,i} \\ V_{k,i} \end{bmatrix} = F \begin{bmatrix} px_{k,i} \\ py_{k,i} \\ V_{k,i} \end{bmatrix} + G\delta_k. \quad (2)$$

Among them, the state transition matrix is expressed as:

$$F = \begin{bmatrix} 1 & 0 & \Delta t \cos \hat{\theta}_{k,i} \\ 0 & 1 & \Delta t \sin \hat{\theta}_{k,i} \\ 0 & 0 & 1 \end{bmatrix}, G = \begin{bmatrix} \Delta t/2 \cos \hat{\theta}_{k,i} \\ \Delta t/2 \sin \hat{\theta}_{k,i} \\ 1 \end{bmatrix} \cdot \Delta t$$

represents the sampling time interval, and $\hat{\theta}_{k,i}$ means the heading angle of the target node i at time t_k . To reduce the computational complexity of multitarget tracking, as argued in [9] and [11], δ_k is a Gaussian random variable with zero mean and covariance γ^2 , that is $\delta_k \sim N(0, \gamma^2)$.

B. Measurement Model

The distance measurement sensor outside the node and the inertial measurement sensor inside the node measures the measurement value during the state transition of the target node. Usually, an accelerometer measures the acceleration, and integrating the acceleration can measure the step size information during the transfer process of the target node. The step size estimate is expressed as

$$\hat{l}_{k,i} = l_{k,i} + \eta_{1,k}. \quad (3)$$

Among them, $l_{k,i}$ represents the real distance that the moving target node i is transferred from the position $(px_{k,i}, py_{k,i})$ at time t_k to the position $(px_{k+1,i}, py_{k+1,i})$ at time t_{k+1} , that is

$$l_{k,i} = \sqrt{(px_{k+1,i} - px_{k,i})^2 + (py_{k+1,i} - py_{k,i})^2}. \quad (4)$$

And $n_{1,k}$ is the step noise obeying a Gaussian distribution. Accordingly, $\hat{l}_k = [\hat{l}_{k,1}, \hat{l}_{k,2}, \dots, \hat{l}_{k,m}]^T$ reflects the step size information of M target nodes at time t_k . The gyroscope measures the angular velocity, and the heading angle during the transfer of the target node can be obtained by integrating the angular velocity. The angle estimate is expressed as

$$\hat{\theta}_{k,i} = \theta_{k,i} + \eta_{2,k} \quad (5)$$

where $\theta_{k,i}$ is the actual horizontal angle, namely

$$\theta_{k,i} = \arctan \frac{py_{k+1,i} - py_{k,i}}{px_{k+1,i} - px_{k,i}} \quad (6)$$

where $n_{2,k}$ is the angular noise following a Gaussian distribution, $\hat{\theta}_k = [\hat{\theta}_{k,1}, \hat{\theta}_{k,2}, \dots, \hat{\theta}_{k,m}]^T$ reflects the angle information of M target nodes at time t_k . Therefore, $Z_k = [\hat{l}_k, \hat{\theta}_k]$ is defined as the inertial measurement inside the node. That is,

the measurement model of the inertial measurement sensor is expressed as follows:

$$Z_k = h(X_k, \vartheta_k) \quad (7)$$

where h represents the nonlinear measurement function and ϑ_k represents the measured deviation value. The distance measurement $\hat{d}_{k,ij}$ between target nodes at time t_k obtained by the TOA ranging method is estimated as

$$\hat{d}_{k,ij} = d_{k,ij} + \eta_{3,k} \quad (8)$$

where d is the actual distance between the target nodes i and j , namely

$$d_{k,ij} = \sqrt{(px_{k,i} - px_{k,j})^2 + (py_{k,i} - py_{k,j})^2} \quad (9)$$

where $n_{3,k}$ is the distance noise obeying a Gaussian distribution, accordingly, $S_k = \{\hat{d}_{k,ij} | j \in \{1, \dots, M\} \setminus \{i\}\}$ reflects the distance information between the target node i and other $M-1$ target nodes at time t_k , that is, the distance measurement outside the node.

III. COOPERATIVE GAUSSIAN CONDENSATION FILTER

In this section, we first describe a GCF based on particle flow to complete the temporal filter estimation of target nodes. Second, a GCF based on cooperatively constrained particle flow is introduced to realize multitarget cooperative tracking.

A. Gaussian Condensation Filter Based on Particle Flow

Under nonideal conditions, this article uses GCF for state estimation to solve the nonlinear problem of the measurement model. However, there is a defect in sampling point degradation in the prediction and update process of GCF. This study proposes a GCF based on PF to solve this problem. The PF represents the continuous change process from the sampling point of the prior distribution to the posterior distribution. In this section, we first introduce the fundamental idea of GCF, describe the ‘‘flow’’ of sampling points, and introduce GCF based on PF to obtain high-precision state estimation information.

1) *Gaussian Condensation Filter*: GCF [17] provides a way to recursively generate the posterior probability density function of the target state. The algorithm estimates the state of the target node and identifies the unknown parameters of the Gaussian mixture model, including three stages of prediction, update, and Gaussian condensation. In the prediction stage, the state prediction of the current moment is carried out according to the prior knowledge of the previous moment. In the update phase, the predicted state is updated by the measured value according to the observation equation, and the posterior estimate of the current moment is obtained. In the Gaussian condensation stage, considering the nonlinearity of the measurement model, the posterior probability density function is first approximated using a Gaussian mixture model. Then this Gaussian mixture distribution is used for target state estimation.

1) *Prediction*: Assume that the target node performs state transition based on the first-order Markov model, that

is, $p(X_k|X_{1:k-1}) = p(X_k|X_{k-1})$ is satisfied. At time t_k , the prior probability distribution $p(X_k|Z_{1:k-1})$ of the target node state can be obtained by the high-dimensional integral of the product of the system state equation $p(X_k|X_{k-1})$ and the prior probability distribution $p(X_{k-1}|Z_{1:k-1})$ at the last moment. However, for non-Gaussian systems, computing the integral is extremely complicated. Only when the posterior probability density function of the last moment is a Gaussian distribution or a Dirac function can the analytical solution of the prior probability density function of the current moment be obtained. That is also the property used by the Kalman filter and particle filter. In addition, according to the central limit theorem, any statistical distribution can be approximated as a Gaussian mixture distribution, and the number of branches of the Gaussian mixture distribution is much smaller than that of the Dirac function [18]. Since the dynamic model is usually a Gaussian system model, the prediction step can be computed in closed form. Based on this, this study considers the target motion tracking problem under the system state equation to be linear, and the posterior probability distribution is a Gaussian mixture model, namely

$$\hat{p}(X_{k-1}|Z_{1:k-1}) = \sum_{i=1}^m \alpha_i N(X_{k-1}; \mu_{k-1|k-1}^{(i)}, Q_{k-1|k-1}^{(i)}). \quad (10)$$

The formula for the prediction stage is expressed as

$$\tilde{p}(X_k|Z_{1:k-1}) = \sum_{i=1}^m \alpha_i N(X_k; \mu_{k|k-1}^{(i)}, Q_{k|k-1}^{(i)}) \quad (11)$$

where $\mu_{k|k-1}^{(i)} = F\mu_{k-1|k-1}^{(i)}$ and $Q_{k|k-1}^{(i)} = FQ_{k-1|k-1}^{(i)}F^T + \gamma^2$ are the mean and covariance of the predicted state, m is the number of mixture Gaussian kernels, and γ^2 is the variance of the process noise δ_k .

- 2) *Update*: The posterior probability density function is updated by the inertial measurement Z_k obtained at time t_k . As shown in Fig. 2, since the likelihood function $p(Z_k|X_k)$ defined by the measurement model $h(X_k)$ is nonlinear, the updated posterior probability distribution $\tilde{p}(X_k|Z_{1:k})$ does not belong to the Gaussian mixture model. According to (11), the formula for the update phase is expressed as

$$\tilde{p}(X_k|Z_{1:k}) \propto p(Z_k|X_k) \sum_{i=1}^m \alpha_i N(X_k; \mu_{k|k-1}^{(i)}, Q_{k|k-1}^{(i)}). \quad (12)$$

- 3) *Gaussian Condensation*: For nonlinear filter algorithms, the number of sufficient statistics describing the actual posterior distribution increases over time [19]. To avoid this, we aggregate the accurate posterior probability distribution into a Gaussian mixture model based on a closed-form idea. Therefore, one can iterate using expectation maximization (EM) [20] estimation to obtain a

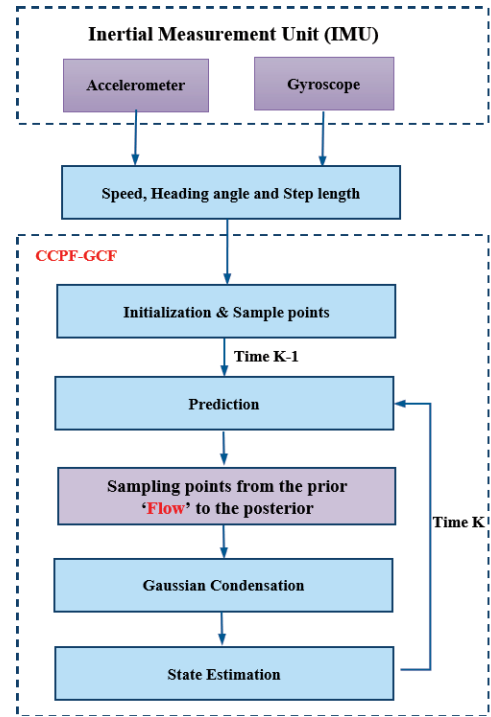


Fig. 2. GCF based on PF flow.

Algorithm 1 GCF

1. **Input**: $\tilde{p}_k \leftarrow$ True Posterior Probability Distribution
2. **Output**: $\{\lambda_k, \hat{p}_k\} \leftarrow$ Gaussian Mixture Distribution
3. $q(X, \lambda^0) = \sum_{i=1}^m \alpha_i^{(0)} N(X; \mu_i^{(0)}, \Sigma_i^{(0)})$
4. Initialization Parameters: $\lambda^0 = (\alpha_1^{(0)}, \dots, \alpha_m^{(0)}, \mu_1^{(0)}, \dots, \mu_m^{(0)}, \Sigma_1^{(0)}, \dots, \Sigma_m^{(0)})$
5. **DO**
6. **FOR** $i \leftarrow 1 : m$ **DO**
7. $f(X) = \alpha_i^{(l)} N(X; \mu_i^{(l)}, \Sigma_i^{(l)}) \tilde{p}_k$
8. $C = \text{sum}(f(X))$
9. $\alpha_i^{(l+1)} = C$
10. $\mu_i^{(l+1)} = \frac{\text{sum}(Xf(X))}{C}$
11. $\Sigma_i^{(l+1)} = \frac{\text{sum}((X - \mu_i^{(l+1)})(X - \mu_i^{(l+1)})^T f(X))}{C}$
12. **ENDFOR**
13. **WHILE** $\lambda^{(l+1)} \neq \lambda^{(l)}$
14. $\hat{p}_k = \sum_{i=1}^m \alpha_i^{(l+1)} N(X; \mu_i^{(l+1)}, \Sigma_i^{(l+1)})$

Gaussian mixture distribution q where the true posterior probability distribution p minimizes the KL divergence [21]. The Gaussian condensation algorithm is described in Algorithm 1.

2) *Particle Flow*: To solve the defect of sampling point degradation in GCF, this study calculates the posterior probability of the target state based on the Bayesian formula to realize the update process. The PF is used to describe the change process from the prior distribution to the posterior distribution by constructing the homotopy function. The PF velocity field is obtained according to the Fokker–Planck equation describing

the probability distribution and then calculated by numerical integration test distribution samples.

Assuming that the posterior probability distribution of the target node is represented by N sampling points $\{x_{k-1}^i\}_{i=1}^N$ at time t_{k-1} , after the state of the sampling points is predicted by the dynamic model, we can obtain the sampling points $\{\tilde{x}_k^i\}_{i=1}^N$ that represent the prior distribution at time t_k . Further, in this study, these sampling points that satisfy the prior distribution of the target node state are moved to the corresponding posterior distribution through PF. We denote η_ϑ as the change of the target state with the time interval $\vartheta \in [0, 1]$, while denoting the change of the state at the i th sampling point by η_ϑ^i and $\eta_0^i = \tilde{x}_k^i$.

In the update stage, this study calculates the posterior probability function of the sampling point $p(\eta_\vartheta^i | Z_{1:k})$ based on the Bayesian formula, which is expressed as

$$p(\eta_\vartheta^i | Z_{1:k}) = \frac{p(\eta_\vartheta^i | Z_{1:k-1})p(Z_k | \eta_\vartheta^i)}{p(Z_k | Z_{1:k-1})}. \quad (13)$$

Denote $g(\eta_\vartheta^i)$ the prior probability density, denote the likelihood function $p(\eta_\vartheta^i | Z_{1:k})$, and $h(\eta_\vartheta^i)$ construct the homotopy function $p(Z_k | \eta_\vartheta^i)$ from (13)

$$p(\eta_\vartheta^i, \vartheta) = \frac{g(\eta_\vartheta^i)h(\eta_\vartheta^i)^\vartheta}{\int g(\eta_\vartheta^i)h(\eta_\vartheta^i)^\vartheta d\eta_\vartheta^i}. \quad (14)$$

Taking the natural logarithm of (14), we get

$$\ln p(\eta_\vartheta^i, \vartheta) = \ln g(\eta_\vartheta^i) + \vartheta \ln h(\eta_\vartheta^i) - \ln K(\vartheta) \quad (15)$$

where $K(\vartheta) = \int g(\eta_\vartheta^i)h(\eta_\vartheta^i)^\vartheta d\eta_\vartheta^i$ represents a state-independent normalization factor. When ϑ changing continuously from 0 to 1, $p(\eta_\vartheta^i, \vartheta)$ represents the probability density function of the sampling point i in the process of changing from the prior distribution ($\vartheta = 0$) to the posterior distribution ($\vartheta = 1$). Assuming that the PF obeys the stochastic differential equation, the rate of change of the state at the sampling point η_ϑ^i is

$$\frac{d\eta_\vartheta^i}{d\vartheta} = \zeta(\eta_\vartheta^i, \vartheta) + \frac{d\sigma}{d\vartheta} \quad (16)$$

where η_ϑ^i the velocity field representing the smooth movement of sampling points from the prior distribution to the posterior distribution, and ϑ is process noise.

Suppose the process noise is 0, and $p(\eta_\vartheta^i, \vartheta)$ satisfies the Fockker–Planck equation of the zero diffusion term, namely

$$\frac{\partial p(\eta_\vartheta^i, \vartheta)}{\partial \vartheta} = -\text{div}(\zeta(\eta_\vartheta^i, \vartheta)p(\eta_\vartheta^i, \vartheta)) \quad (17)$$

where div indicates the divergence. Therefore, after calculating $\zeta(\eta_\vartheta^i, \vartheta)$ from the above formula, the sampling points that satisfy the posterior distribution are obtained by integrating $\zeta(\eta_\vartheta^i, \vartheta)$ from 0 to 1. The localized exact Daum and Huang (LEDH) filter algorithm obtain the analytical solution of the velocity field for each sampling point. For the i th sampling point, the PF velocity field is expressed as

$$\zeta(\eta_\vartheta^i, \vartheta) = A^i(\vartheta)\eta_\vartheta^i + b^i(\vartheta) \quad (18)$$

$$A^i(\vartheta) = -\frac{1}{2}QH^i\vartheta^T(\vartheta H^i\vartheta QH^i\vartheta^T + R)^{-1}H^i(\vartheta) \quad (19)$$

Algorithm 2 Particle Flow

1. Input: $\{x_{k-1}^i\}_{i=1}^N \leftarrow N$ sampling points at time t_{k-1}
2. $\{Q_k^{(n)}\}_{n=1}^m \leftarrow$ Prediction covariance
3. Output: $\{\eta^i\}_{i=1}^N \leftarrow N$ sampling points at time t_k
4. **FOR** $i = 1, N$ **DO**
5. $\tilde{\eta}_0^i = f_1(x_{k-1}^i, 0) \leftarrow$ State Transition Function
6. $\eta^i = f_1(x_{k-1}^i, \delta)_k$
7. $\tilde{\eta}^i = \tilde{\eta}_0^i$
8. **ENDFOR**
9. $\vartheta = 0$
10. **FOR** $j = 1 : N_\vartheta$ **DO**
11. $\vartheta = \vartheta + \xi_j$
12. **FOR** $i = 1 : N$ **DO**
13. $\frac{H^i(\vartheta) = \partial h(\tilde{\eta}^i, 0)}{\partial \tilde{\eta}^i} \leftarrow$ Observation Matrix
14. $e^i(\vartheta) = h(\tilde{\eta}^i, 0) - H^i(\vartheta)\tilde{\eta}^i \leftarrow$ Truncation error
15. $A^i(\vartheta) = -\frac{1}{2}QH^i\vartheta^T(\vartheta H^i\vartheta QH^i\vartheta^T + R)^{-1}H^i(\vartheta)$
16. $b^i(\vartheta) = (I + 2\vartheta A^i\vartheta)[I + \vartheta H^i\vartheta QH^i\vartheta^T R^{-1}(Z_k - e^i(\vartheta)) + A^i\vartheta\tilde{\eta}_0^i]$
17. $\tilde{\eta}^i = \tilde{\eta}^i + \varepsilon_j(A_j^i(\vartheta)\tilde{\eta}^i + b_j^i(\vartheta))$
18. $\eta^i = \eta^i + \varepsilon_j(A_j^i(\vartheta)\eta^i + b_j^i(\vartheta))$
19. **ENDFOR**
20. **ENDFOR**

$$b^i(\vartheta) = (I + 2\vartheta A^i\vartheta) \times \left[I + \vartheta H^i\vartheta QH^i\vartheta^T R^{-1}(Z_k - e^i(\vartheta)) + A^i\vartheta\tilde{\eta}_0^i \right] \quad (20)$$

where Q represents the covariance of the predicted state, I represents the identity matrix. H represents the measurement equation linearized by the nonlinear function h at η_ϑ^i , that is, $H^i(\vartheta) = ([\partial h(\eta, 0)]/\partial \eta)|_{\eta = \eta_\vartheta^i}$, $h(\eta_\vartheta^i, v) \sim N(H\eta_\vartheta^i, R)$ and $e^i(\vartheta) = h(\eta_\vartheta^i, 0) - H^i(\vartheta)\eta_\vartheta^i$, and $\tilde{\eta}_0^i$ represent the sampling point i when the process noise is zero through the dynamic state of the model after transfer. Only when the prior distribution $g(\eta_\vartheta^i)$ and the measurement function $h(\eta_\vartheta^i)$ are both Gaussian distributions can the exact solution of the particle flow velocity field be obtained. But LEDH filter relies on an extended Kalman filter or UKF to calculate PF velocity field. When the measurement model is highly nonlinear, the performance of the traditional Kalman filter is not good. Therefore, we propose a GCF based on PF, which uses a Gaussian mixture distribution to approximate the posterior distribution of the target node state to obtain the updated state covariance. The PF algorithm is detailed in Algorithm 2.

3) *Gaussian Condensation Filter Based on Particle Flow*: This study proposes a GCF algorithm based on PF, and the algorithm flowchart is shown in Fig. 2. Assume that the posterior probability distribution $\{\mu_{k-1}^{(n)}, Q_{k-1}^{(n)}\}_{n=1}^m$ approximates a Gaussian mixture distribution $\{x_{k-1}^i\}_{i=1}^N$ at time t_{k-1} . In the prediction stage, the state of the sampling point at the current moment is predicted according to the dynamic model, and the mean and variance $\{\mu_k^{(n)}, Q_k^{(n)}\}_{n=1}^m$ of the predicted state is obtained. In the update stage, the posterior samples can be obtained from the prior samples by solving the velocity field through the PF mechanism. Therefore, we can get the sampling point $\{x_k^i\}_{i=1}^N$ that obeys the posterior distribution of the state of

Algorithm 3 PF-GCF

1. Input: $[X_0] \leftarrow$ Initial position
2. Output: $\{\hat{X}_k\}_{k=1}^K \leftarrow$ The estimate of state
3. Initialization Parameters: $\{x_0\}_{i=1}^N \sim \hat{p}_0 \leftarrow$ The prior distribution of X_0 and $\hat{p}_0 \sim N(\mu_0, Q_0)$
4. **FOR** $k = 1 : K$ **DO**
5. **FOR** $n = 1 : m$ **DO**
6. $\mu_k^{(n)} = F\mu_{k-1}^{(n)}$
7. $Q_k^{(n)} = FQ_{k-1}^{(n)}F + \gamma^2$
8. **ENDFOR**
9. **IF** $x_{k-1}^i \sim N(\mu_{k-1}^{(n)}, Q_{k-1}^{(n)})$ **THEN**
10. $\{x_k^i\}_{i=1}^N \leftarrow PF(\{x_{k-1}^i\}_{i=1}^N, \{Q_k^{(n)}\}_{n=1}^m) \triangleleft$ Algorithm: Particle Flow
11. **ENDIF**
12. $\hat{X}_k = \frac{1}{N} \sum_{i=1}^N x_k^i \triangleleft$ The estimate value of state
13. $\hat{p}_k \leftarrow GCF(\{x_k^i\}_{i=1}^N) \triangleleft$ Algorithm: Gaussian Condensation Filter

the target node. Then use the state mean $\hat{X}_k = (1/N) \sum_{i=1}^N x_k^i$ of the sampling points as the estimated value of the target node's state at time t_k to obtain its position in the time series.

Considering the infinite increase of sufficient statistics to describe the true posterior \tilde{p} with time series changes, we approximate \tilde{p} to a Gaussian mixture distribution \hat{p} using Gaussian condensation theory. It uses EM to estimate the unknown parameters in the Gaussian mixture model to obtain the updated state covariance. The Gaussian condensation algorithm based on PF is described in Algorithm 3.

B. Co-Optimization Method Based on Distance Constraints

Bayesian estimation is to predict and update the posterior probability density distribution recursively, and the state estimation bias of previous moments affects the state estimation of subsequent moments. To effectively reduce the influence of the cumulative positioning error, this study integrates the distance measurement information between target nodes for co-location estimation. In the co-location tracking method, the Bayesian optimization method under the distance constraint is used in this study to optimize the estimation of the target node state. The GCF based on error elliptical PF will output the mean and covariance of the target node state at each moment. This information is used as the input of the constrained optimization estimation. Under the distance constraint of the given target node state, this study uses the deterministic sampling approximation. Calculating the integral obtains the posterior conditional mean and covariance to realize the multitarget tracking under the distance constraint.

In this study, the Gaussian filter algorithm based on error ellipse PF is used to estimate the state of the mobile node, and the target node obtains the information gain of the inertial sequence data in time. Next, we use the distance between the two target nodes as mutual information to suppress the influence of cumulative errors in single-target tracking, thereby achieving higher precision multitarget co-location. The algorithm flowchart is shown in Fig. 3.

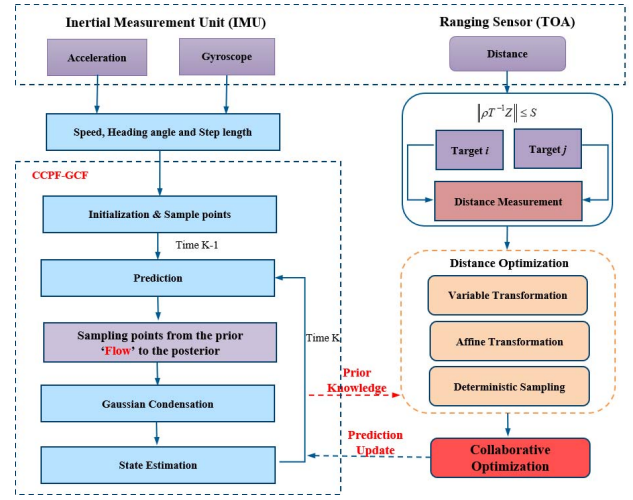


Fig. 3. PF-GCF.

For single-target tracking, during the resampling stage, particle flow-based GCF (PF-GCF) could be further improved by our previous method [14], contributing to the error-elliptical particle flow-based GCF (EPF-GCF). First, input the initial position information of the target node and complete the initial generation of sampling points. Second, the dynamic model predicts the state of the sampling points. The PF velocity field is calculated according to the variance $\{Q_k^{(n)}\}_{n=1}^m$ of the predicted state. These sampling points are smoothly migrated from the prior distribution to the posterior distribution by integrating the velocity field from 0 to 1. Then, according to the state estimated value of “flowing” to the sampling points of the posterior distribution as the center point (x_p, y_p) of the sampling point set. Given an error ellipse with a confidence level of 3σ , the abnormal sampling points outside the error ellipse are directly discarded. In the ellipse, the corresponding number of sampling points is selected for copying to ensure that the sample size of the corrected sampling points is conserved. Finally, the Gaussian condensation method is used to iterate continuously until the optimal solution of the parameters in EM is reached, and the covariance of the updated state is obtained to complete the rough estimation of the target node state.

In the multitarget-tracking process, the state estimation of GCF based on error elliptical PF will be used as the input of distance-constrained optimization. In the collaborative network, the target node establishes a distance constraint c based on its prior knowledge at the last moment and the distance information between nodes. It obtains the estimated value $\hat{u}_{r|c}$ of the state through the distance constraint optimization algorithm, which is closer to the actual state vector. Therefore, this study considers using the state estimation after the distance constraint optimization to construct the error ellipse. That is, the state estimation $\hat{u}_{r|c}$ after the constraint optimization is used to update the center point (x_p, y_p) of the error ellipse at the next moment. Then the GCF estimation at the next moment can obtain at the last moment. The gain of distance information at a time can realize high-precision multitarget co-location based on IMU/TOA information fusion. For a detailed description of

Algorithm 4 CCPF-GCF

```

1. Input:  $[X_0] \leftarrow$  Initial position
2. Output:  $\{\hat{u}_{r1|c}\}_{k=1}^K \leftarrow$  The estimate value of state
3. Initialization Parameters:  $\{x_0\}_{i=1}^N \sim \hat{p}_0 \leftarrow$  The prior distribution of  $X_0$  and  $\hat{p}_0 \sim N(\mu_0, Q_0)$ 
4. FOR  $k = 1 : K$  DO
5.   FOR  $n = 1 : m$  DO
6.      $\mu_k^{(n)} = F\mu_{k-1}^{(n)}$ 
7.      $Q_k^{(n)} = FQ_{k-1}^{(n)}F + \gamma^2$ 
8.   ENDFOR
9.   IF  $x_{k-1}^i \sim N(\mu_{k-1}^{(n)}, Q_{k-1}^{(n)})$  THEN
10.     $\{x_k^i\}_{i=1}^N \leftarrow PF(\{x_{k-1}^i\}_{i=1}^N, \{Q_k^{(n)}\}_{n=1}^m) \triangleleft$  Algorithm: Particle Flow
11.   ENDIF
12.    $\hat{X}_k = \frac{1}{N} \sum_{i=1}^N x_k^i \leftarrow$  The estimate value of state
13.    $\{x_k^i\}_{i=1}^N \leftarrow EEO(\{x_k^i\}_{i=1}^N, (x_p, y_p)) \triangleleft$  Algorithm: Error Ellipse Optimization
14.    $\hat{p}_k \leftarrow GCF(\{x_k^i\}_{i=1}^N) \triangleleft$  Algorithm: Gaussian Condensation Filter
15.    $u_1 = \hat{X}_k, C_1 = cov(\{x_k^i\}_{i=1}^N) \triangleleft$  The mean and variance of current sampling time
16.    $u_r = [u_1, u_2]^T, C_r = [C_1, C_2]^T$ 
17.    $\hat{u}_{r1|c}, \hat{C}_{r1|c}, \hat{C}_{r2|c} \leftarrow DCO(u_r, C_r, S_{12}) \triangleleft$  Distance constrained optimization
18.    $(x_p, y_p) \leftarrow f_1(\hat{u}_{r1|c}) \triangleleft$  Update the estimate center of next sampling time
19. ENDFOR

```

the error ellipse and distance-constrained optimization algorithms, please refer to [22]. The multiobjective cooperative Gaussian condensation description is shown in Algorithm 4.

IV. NUMERICAL SIMULATION AND ANALYSIS

A. Experimental Environment and Parameter Settings

In the simulation stage, this article conducts the positioning and tracking experiment of target node walking based on MATLAB. The personal computer hardware is configured as a 4-core Intel i5 CPU and 8-GB RAM, and the operating system is Win 10 Home Edition 64-bit. Set the motion scene of the target node as a square area with a length of 50 m and a width of 50 m. To ensure that the motion law of the mobile node conforms to the dynamic random walk process, the initial position (x_0, y_0) and the motion heading angle θ of the target node of each experiment are randomly set. And 100 steps are randomly traveled within a 2-D scene of 50 m \times 50 m. The experimental parameters of location tracking are shown in Table I.

B. Algorithm Performance Statistics and Analysis

In this article, a GCF algorithm based on PF is proposed to estimate the system state effectively to improve the positioning accuracy of the nonlinear filter algorithm in single target tracking. To verify the high precision and stability of proposed algorithms, this study uses UKF, particle filter, GCF, PF-GCF, and EPF-GCF to conduct single-target tracking. Repeat

TABLE I
EXPERIMENTAL PARAMETER SETTINGS

Parameter	Value (unit)
Sampling Interval Δt	1(s)
Process Noise	1(m^2)
Variance γ^2	1(m^2)
Velocity V	2(m/s)
Step Noise $n_{1,k}$	0.1(m^2)
Angle Noise $n_{2,k}$	5($^\circ$)
Distance Measurement	0.5(m^2)
Noise $n_{3,k}$	0.5(m^2)
Mixed Gaussian	8
Kernels m	8
Sampling Point N	4000

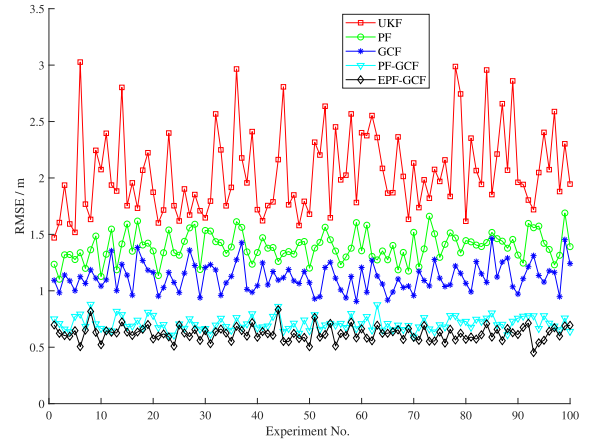


Fig. 4. RMSE distribution of different algorithms for single target tracking.

the above algorithms 100 times, and calculate the root mean square error, defined as

$$RMSE = \sqrt{\frac{1}{K} \sum_{i=1}^K e^2}. \quad (21)$$

Fig. 4 shows different positioning algorithms' root mean square error distribution under single target tracking. From the statistics of the results, we can see that

- 1) The simulation result of the UKF is poor, and there is a significant oscillation phenomenon. The root mean square error distribution of the particle filter and GCF is close, but the GCF is more stable and has higher positioning accuracy. This shows that the GCF algorithm has the advantage of improving the localization performance in dealing with the nonlinearity of the measurement model.
- 2) The error curve of GCF based on PF is significantly lower than that of the GCF. Compared with the GCF, the positioning performance is improved by 36.7%, with obvious advantages in estimation accuracy and stability.
- 3) Compared with the GCF based on PF, the GCF based on error ellipse optimization has a smaller error distribution. As the iteration progresses, the EPF-GCF algorithm suppresses the influence of the previous error to a certain extent. This proves that the algorithm described in this

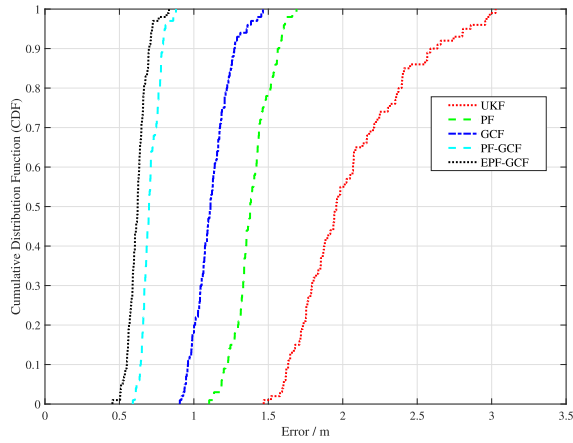


Fig. 5. RMSE CDF of different algorithms for single target tracking.

article can effectively improve the positioning accuracy of single-target tracking.

The cumulative distribution function curves of the root mean square error of different algorithms under single target tracking are shown in Fig. 5. The following conclusions can be drawn from the analysis of the figure: the positioning accuracy of the GCF is higher than 0.9 m. The GCF based on PF has a 52% probability of being lower than 0.7 m. The GCF of PF is optimized based on the error ellipse. The positioning accuracy of the algorithm has a 90% probability lower than 0.7 m, which also verifies the effectiveness of the GCF based on error ellipse optimization PF in single target tracking.

The multitarget cooperative tracking algorithm fuses the distance information gained between nodes to obtain higher precision positioning and tracking. To verify the effectiveness of the GCF based on cooperatively constrained particle flow in target tracking, this study uses the cooperative particle filter (CPF), the CGCF, and the cooperative constrained particle flow-based GCF (CCPF-GCF) repeats 100 random walk experiments and counts the root mean square error, defined as

$$\text{CRMSE} = \frac{1}{M} \sum_{i=1}^M \sqrt{\frac{1}{K} \sum_{j=1}^K e^2}. \quad (22)$$

Then, to further verify the advancement of the algorithm proposed in this article in target tracking, the error distributions of the above algorithms are compared with the collaborative PCRLB with the same measurement noise. The statistics of the results are shown in Fig. 6.

Fig. 6 shows different algorithms' root mean square error distribution under multitarget tracking. The following conclusions can be obtained from the result statistics.

- 1) The synergistic root means square error curves of the above-mentioned collaborative algorithms are relatively stable, which indicates that the multiobjective collaborative technology effectively integrates the position information of a single target and verifies that the multiobjective collaborative algorithm has higher stability.
- 2) The positioning accuracy of the CPF algorithm is 0.39 m, the positioning accuracy of the CGCF algorithm

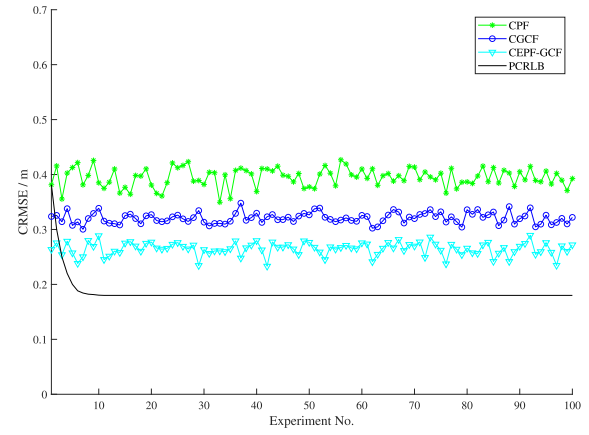


Fig. 6. CRMSE distribution of different algorithms for multitarget tracking.

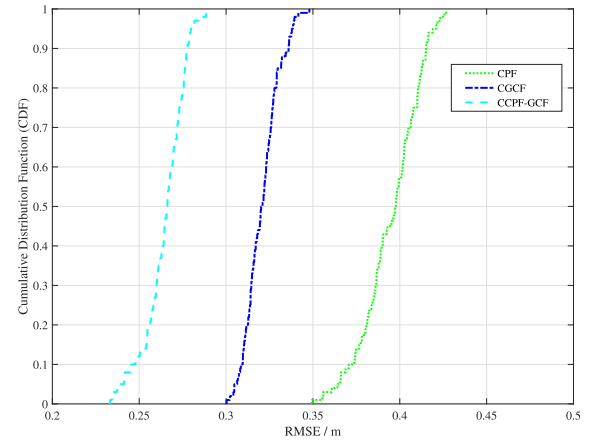


Fig. 7. CRMSE CDF of different algorithms for multitarget tracking.

is 0.32 m, and the positioning accuracy of the CCPF-GCF algorithm is 0.26 m. Compared with CGCF, CCPF-GCF has higher positioning accuracy, and the root means square error curve of the CCPF-GCF algorithm is closer to that of the collaborative PCRLB. The effectiveness of the proposed GCF based on cooperative constrained PF in cooperative motion tracking is verified.

Fig. 7 shows the cumulative distribution function curve of different algorithms' root mean square error under multitarget tracking. From the analysis of the figure, the positioning accuracy of CPF is below 0.45 m, the positioning accuracy of CGCF is below 0.35 m, and the positioning accuracy of CCPF-GCF is 0.3 m. This also verifies that the CCPF-GCF algorithm proposed in this article can achieve higher precision multitarget cooperative tracking.

This study uses the nonlinear filter for single-target and co-location simulation experiments. Table II summarizes the positioning error and execution time of different algorithms. The following conclusions can be drawn from the table.

- 1) In the single-target tracking algorithm, GCF can achieve a positioning accuracy of 1.12 m in single-target tracking. Compared with the UKF and PF algorithms, the GCF algorithm has higher positioning accuracy. Second, GCF's running time is higher than UKF due to the iterative solution required by the GCF algorithm in the Gaussian condensation stage. However, the running

TABLE II
POSITIONING ACCURACY OF DIFFERENT ALGORITHMS (4000 SAMPLING POINTS)

Algorithm	Max Error(m)	Min Error(m)	Avg Error(m)	Execution Time(s)
UKF	3.02	1.47	2.05	0.06
PF	1.69	1.10	1.39	0.15
GCF	1.46	0.91	1.12	0.12
PF-GCF	0.88	0.59	0.71	0.17
EPF-GCF	0.83	0.45	0.62	0.18
CPF	0.43	0.35	0.39	0.19
CGCF	0.35	0.30	0.32	0.16
CCPF-GCF	0.29	0.23	0.26	0.22

time of GCF is lower than that of PF, which indicates that GCF is computationally less expensive in high-dimensional states.

- 2) Compared with the GCF algorithm, PF-GCF provides higher positioning accuracy and minor variance, which proves that PF-GCF effectively improves the problem of sampling point degradation. EPF-GCF can achieve a positioning accuracy of 0.62 m in single target tracking. Since the error ellipse optimization needs to filter the sampling points, the running time of the EPF-GCF algorithm is slightly higher. Still, it is entirely acceptable for real-time applications.
- 3) In the multitarget cooperative tracking algorithm, CCPF-GCF can achieve a positioning accuracy of 0.26 m. CCPF-GCF dramatically improves positioning accuracy and stability than the single target-tracking algorithm.

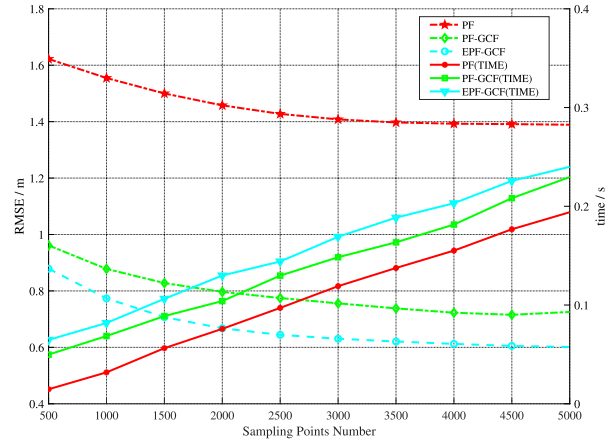


Fig. 8. Influence of the number of sampling points on the localization performance of the algorithm.

C. Effect of Parameter Settings on Algorithm Performance

To further analyze the influence of the number of sampling points on the localization performance of different algorithms, this study uses particle filter, PF GCF (PF-GCF), and error ellipse optimization PF GCF algorithm (EPF-GCF) for simulation experiments. The positioning accuracy of the algorithm is represented by the root mean square error. In addition, the effect of the number of sampling points on the execution time of different filter is compared, and the statistics of the results are shown in Fig. 8. The following conclusions can be drawn from the figure. As the number of sampling points increases, the positioning error gradually decreases, but the time cost increases linearly when the number of sampling points is less than 4000. As the number of sampling points increases, the algorithm’s accuracy is improved. When the number of sampling points is more significant than 4000, with the rise in the number of sampling points, the change of the positioning error is relatively stable. Therefore, considering the marginal cost of positioning accuracy and execution efficiency, an appropriate number of sampling points should be selected.

Next, we discuss the effect of noise variance on the localization performance of the algorithm. Selecting different measurement noise covariances, using particle filter, GCF, PF-GCF, and the proposed error ellipse optimization particle flow-based GCF (EPF-GCF) algorithm repeat 100 random walk experiments, and the statistics of the results are shown in Fig. 9. The figure shows that the positioning error increases

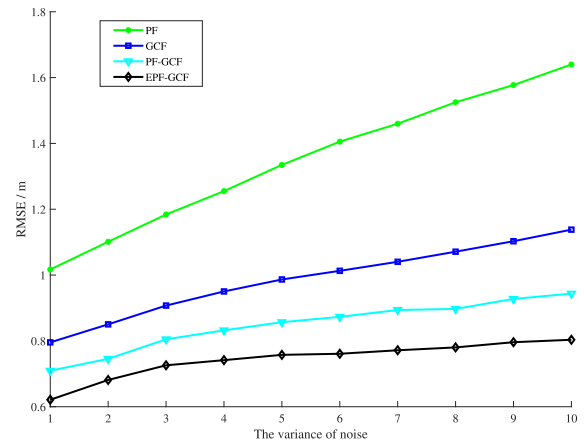


Fig. 9. Influence of noise variance on localization performance of the algorithm.

with noise variance. Compared with the contrast filter, EPF-GCF has higher accuracy and is less affected by the noise variance.

To analyze the influence of the number of target nodes on the performance of different algorithms, simulation results are shown in Fig. 10, from which it can be seen that:

- 1) With the increase of target nodes, the positioning error of CCPF-GCF changes more smoothly and accurate. Therefore, when the number of targets is large, CCPF-GCF is effective and suitable for large-scale deployment applications.

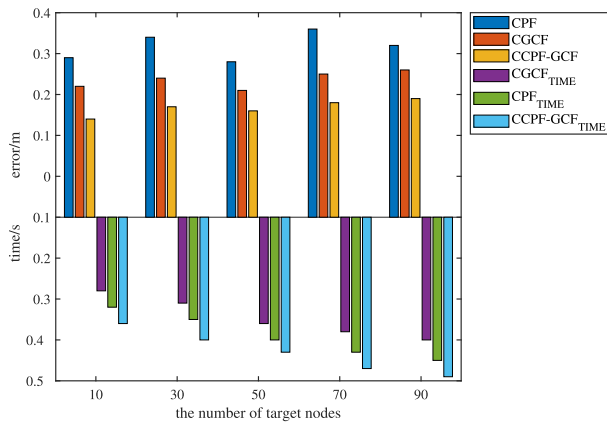


Fig. 10. Influence of the number of target nodes on the algorithm's performance.

- 2) With the increase of target nodes, the execution time of the above algorithms gradually increase, and the execution time of CCPF-GCF is slightly higher than those of comparison algorithms. Still, it can meet the real-time requirements of general systems.

V. CONCLUSION

For the nonlinear problem of the measurement model faced by multitarget tracking, a Gaussian condensation algorithm is proposed in this article. In the Gaussian condensation stage, the unknown parameters of the mixture Gaussian model are adjusted by a recursive, iterative method. The Gaussian mixture model approximates the actual posterior probability distribution. Aiming at the problem of sampling point degradation in GCF, this article proposes a GCF based on particle flow. The particle flow mechanism completes the Bayesian estimation by constructing a homotopy function. These sampling points are smoothly moved from the prior distribution in the state space to the posterior distribution in the state space. Compared with other nonlinear filters, the experimental results show that our proposed CCPF-GCF algorithm can effectively solve the nonlinear problem of the measurement model in the high-dimensional state and deal with the defect of sampling point degradation. Compared with EPF-GCF, the localization accuracy of CCPF-GCF is improved by 58.1%. Compared with CPF, the accuracy of CCPF-GCF is enhanced by 33.3%.

Promising directions for future research are to improve the dynamic model uncertainty. The dynamic model is generally considered a Gaussian model to reduce the computational complexity of multitarget tracking. Even though based on the non-Gaussian hypothesis, it generally needs to reduce the dimensionality of the multitarget tracking process by mapping it to Gaussian space for computation due to the complexity of data association. This article focuses on the measurement model issue, but we may focus on generalizing the dynamic model using numerical methods in our future study.

REFERENCES

- [1] N. Saeed, H. Nam, T. Y. Al-Naffouri, and M.-S. Alouini, "A state-of-the-art survey on multidimensional scaling-based localization techniques," *IEEE Commun. Surveys Tuts.*, vol. 21, no. 4, pp. 3565–3583, 4th Quart., 2019.
- [2] Y. Zou and H. Liu, "Semidefinite programming methods for alleviating clock synchronization bias and sensor position errors in TDOA localization," *IEEE Signal Process. Lett.*, vol. 27, pp. 241–245, Feb. 2020.
- [3] H.-T. Sheng, W.-R. Wu, W.-H. Hsiao, and M. Seretnyk, "Joint channel and AoA estimation in OFDM systems: One channel tap with multiple AoAs problem," *IEEE Commun. Lett.*, vol. 25, pp. 2245–2249, Jul. 2021.
- [4] S. Duan, R. Su, C. Xu, Y. Chen, and J. He, "Ultra-wideband radio channel characteristics for near-ground swarm robots communication," *IEEE Trans. Wireless Commun.*, vol. 19, pp. 4715–4726, Jul. 2020.
- [5] H. Obeidat, W. Shuaieb, O. Obeidat, and R. Abd-Alhameed, "A review of indoor localization techniques and wireless technologies," *Wireless Pers. Commun.*, vol. 119, no. 1, pp. 289–327, 2021.
- [6] C. Xu, D. Chai, J. He, X. Zhang, and S. Duan, "InnoHAR: A deep neural network for complex human activity recognition," *IEEE Access*, vol. 7, pp. 9893–9902, 2019.
- [7] C. Xu, J. He, Y. Li, X. Zhang, X. Zhou, and S. Duan, "Optimal estimation and fundamental limits for target Localization using IMU/TOA fusion method," *IEEE Access*, vol. 7, pp. 28124–28136, 2019.
- [8] Y. Bar-Shalom and W. D. Blair, *Multitarget-Multisensor Tracking: Applications and Advances*. Boston, MA, USA: Artech House, 2000. [Online]. Available: <https://us.artechhouse.com/Multitarget-Multisensor-Tracking-Applications-and-Advances-Volume-3-P1074.aspx>
- [9] B. Copp and K. Subbarao, "Nonlinear adaptive filtering in terrain-referenced navigation," *IEEE Trans. Aerosp. Electron. Syst.*, vol. 51, no. 4, pp. 3461–3469, Oct. 2015.
- [10] J. Uhlmann, "Introduction to the algorithmics of data association in multiple-target tracking," in *Handbook of Multisensor Data Fusion*. Boca Raton, FL, USA: CRC Press, 2017, pp. 89–108.
- [11] N. Bergman, L. Ljung, and F. Gustafsson, "Terrain navigation using Bayesian statistics," *IEEE Control Syst.*, vol. 19, no. 3, pp. 33–40, Jun. 1999.
- [12] C. Rosato, L. Devlin, V. Beraud, P. Horridge, T. B. Schon, and S. Maskell, "Efficient learning of the parameters of non-linear models using differentiable resampling in particle filters," *IEEE Trans. Signal Process.*, vol. 70, pp. 3676–3692, Jul. 2022.
- [13] W. You, F. Li, L. Liao, and M. Huang, "Data fusion of UWB and IMU based on unscented Kalman filter for indoor localization of quadrotor UAV," *IEEE Access*, vol. 8, pp. 64971–64981, 2020.
- [14] X. Wang, C. Xu, S. Duan, and J. Wan, "Error-ellipse-resampling-based particle filtering algorithm for target tracking," *IEEE Sensors J.*, vol. 20, no. 10, pp. 5389–5397, May 2020.
- [15] A. S. Aguiar, F. N. Dos Santos, H. Sobreira, J. B. Cunha, and A. J. Sousa, "Particle filter refinement based on clustering procedures for high-dimensional localization and mapping systems," *Robot. Auton. Syst.*, vol. 137, Mar. 2021, Art. no. 103725.
- [16] Y. Fan, K. Ding, X. Qi, and L. Liu, "Cooperative localization of 3D mobile networks via relative distance and velocity measurement," *IEEE Commun. Lett.*, vol. 25, no. 9, pp. 2899–2903, Sep. 2021.
- [17] R. Fan, R. Huang, and R. Diao, "Gaussian mixture model-based ensemble Kalman filter for machine parameter calibration," *IEEE Trans. Energy Convers.*, vol. 33, no. 3, pp. 1597–1599, Sep. 2018.
- [18] J. Sirignano and K. Spiliopoulos, "Mean field analysis of neural networks: A central limit theorem," *Stochast. Processes Appl.*, vol. 130, no. 3, pp. 1820–1852, 2020.
- [19] T. Northardt and S. C. Nardone, "Track-before-detect bearings-only localization performance in complex passive sonar scenarios: A case study," *IEEE J. Ocean. Eng.*, vol. 44, no. 2, pp. 482–491, Apr. 2019.
- [20] X. Zhu, K. Guo, S. Ren, B. Hu, M. Hu, and H. Fang, "Lightweight image super-resolution with expectation-maximization attention mechanism," *IEEE Trans. Circuits Syst. Video Technol.*, vol. 32, no. 3, pp. 1273–1284, Mar. 2022.
- [21] C. Xu, H. Wu, and S. Duan, "Constrained Gaussian condensation filter for cooperative target tracking," *IEEE Internet Things J.*, vol. 9, no. 3, pp. 1861–1874, Feb. 2022.
- [22] C. Xu, X. Wang, S. Duan, and J. Wan, "Spatial-temporal constrained particle filter for cooperative target tracking," *J. Netw. Comput. Appl.*, vol. 176, Feb. 2021, Art. no. 102913.

Ran Wang (Graduate Student Member, IEEE) received the B.E. degree from Beijing Information Science and Technology University, Beijing, China, in 2013, and the M.S. degree from the University of Science and Technology Beijing, Beijing, in 2016, where she is currently pursuing the Doctoral degree. Her research interests include collaborative positioning, quantum optimization, distributed security, and Internet of Things.

Cheng Xu (Member, IEEE) received the B.E., M.S., and Ph.D. degrees from the University of Science and Technology Beijing, Beijing, China, in 2012, 2015, and 2019, respectively.

He is currently an Associate Professor with the School of Computer and Communication Engineering, University of Science and Technology Beijing. He is supported by the Postdoctoral Innovative Talent Support Program from Chinese Government in 2019. His current research interests include swarm intelligence, multiagent reinforcement learning, multimodal navigation, and Internet of Things.

Dr. Xu is an Associate Editor of the *International Journal of Wireless Information Networks*.

Hang Wu received the master's degree from the University of Science and Technology Beijing, Beijing, China, in 2022.

Her research interests include wireless indoor positioning, pattern recognition, and Internet of Things.

Yuchen Shi is currently pursuing the master's degree with the University of Science and Technology Beijing, Beijing, China.

His research interests include wireless indoor positioning, pattern recognition, and Internet of Things.

Shihong Duan received the Ph.D. degree in computer science from the University of Science and Technology Beijing, Beijing, China.

She is an Associate Professor with the School of Computer and Communication Engineering, University of Science and Technology Beijing. Her research interests include multiagent reinforcement learning, multimodal navigation, and Internet of Things.

Xiaotong Zhang (Senior Member, IEEE) received the M.S. and Ph.D. degrees from the University of Science and Technology Beijing, Beijing, China, in 1997 and 2000, respectively.

He is currently a Professor with the School of Computer and Communication Engineering, University of Science and Technology Beijing. His research interests include quantum optimization, multimodal navigation, and Internet of Things.